2018

Investigation on the optimal cooling tower input capacity of a cooling tower assisted ground source heat pump system

Xuemei Gong
Zhejiang University, xgong@uow.edu.au

Lei Xia
University of Wollongong, lx873@uowmail.edu.au

Zhenjun Ma
University of Wollongong, zhenjun@uow.edu.au

Guangming Chen
Zhejiang University

Lili Wei
Ningbo University

Investigation on the optimal cooling tower input capacity of a cooling tower assisted ground source heat pump system

Abstract

Coupling auxiliary cooling devices with ground source heat pump (GSHP) systems in cooling dominated areas can effectively solve the ground thermal imbalance problem. However, the input capacity of the auxiliary heat rejecter directly affects the performance of such hybrid ground source heat pump (HGSHP) systems. This paper presents an investigation on the optimal cooling tower input capacity of a cooling tower assisted GSHP system through both experiments and simulations. The experiments were carried out based on a HGSHP system implemented in an office building and the experimental results were used to validate a numerical model. A simulation system of the cooling tower assisted GSHP system was then developed using TRNSYS and validated against the experimental data collected. The impacts of the cooling tower input capacity on the soil temperature and the system performance were simulated. The results showed that the soil heat accumulation could be effectively alleviated when the cooling tower input capacity ratio (CTICR) was greater than 50%. The optimal cooling tower input capacity was highly dependent on the operation scenario used. The optimal CTICR under two operation scenarios considered was around 54%, while that under the other operation scenarios was around 63%. The control strategy based on the fixed temperature difference between the cooling water leaving the heat pump and the ambient air dry-bulb temperature was found to be the optimal control strategy for the system studied.

Disciplines

Engineering | Science and Technology Studies

Publication Details

Gong, X., Xia, L., Ma, Z., Chen, G. & Wei, L. (2018). Investigation on the optimal cooling tower input capacity of a cooling tower assisted ground source heat pump system. Energy and Buildings, 174 239-253.

Investigation on the optimal cooling tower input capacity of a cooling tower assisted ground source heat pump system

Xuemei Gong[a], Lei Xia[b,*], Zhenjun Ma[b], Guangming Chen[c], Lili Wei[a]

[a] Building Energy Conservation Research Institute, Ningbo University of technology, 315211, China

[b] Sustainable Buildings Research Centre, University of Wollongong, NSW, 2522, Australia

[c] Institute of Refrigeration and Cryogenics, State Key Laboratory of Clean Energy Utilization, Zhejiang University, 310058, China

*Email: lx873@uowmail.edu.au

Abstract: Coupling auxiliary cooling devices with ground source heat pump (GSHP) systems in cooling dominated areas can effectively solve the ground thermal imbalance problem. However, the input capacity of the auxiliary heat rejecter directly affects the performance of such hybrid ground source heat pump (HGSHP) systems. This paper presents an investigation on the optimal cooling tower input capacity of a cooling tower assisted GSHP system through both experiments and simulations. The experiments were carried out based on a HGSHP system implemented in an office building and the experimental results were used to validate a numerical model. A simulation system of the cooling tower assisted GSHP system was then developed using TRNSYS and validated against the experimental data collected. The impacts of the cooling tower input capacity on the soil temperature and the system performance were simulated. The results showed that the soil heat accumulation could be effectively alleviated when the cooling tower input capacity ratio (CTICR) was greater than 50%. The optimal cooling tower input capacity was highly dependent on the operation scenario used. The optimal CTICR under two operation scenarios considered was around 54%, while that under the other operation scenarios was around 63%. The control strategy based on the fixed temperature difference between the cooling water

leaving the heat pump and the ambient air dry-bulb temperature was found to be the optimal control strategy for the system studied.

Keywords: Hybrid ground source heat pump; Experiment; Simulation; Cooling tower; Input capacity ratio; Control strategy.

Nomenclature

C	specific heat (kJ/(kg K))
D	regression coefficient
f.s	full scale
G	flow rate (L/s)
g	gravity acceleration (kg m/s^2)
H	pump head (m)
Q	Accumulated heat dissipation or heat quantity (kJ)
$\dot{Q}$	heat dissipation rate (kW)
rdg	reading
T	temperature (^{o}C)
W	accumulated power consumption (kWh)
w	transient power consumption (W)
β	correction coefficient
η	efficiency
ρ	density (kg/m^3)

Subscripts

a	actual condition
aux	auxiliary cooling system
b	borehole wall
d	daily
des	design
e	end
ET	fixed entering temperature control strategy
f	auxiliary heat dissipation
g	ground heat exchanger
gi	inlet water of the ground heat exchanger
go	outlet water of the ground heat exchanger

HP	heat pump
i	initial
in	inlet
p	pump
RT	fixed running time control strategy
r	rated condition
s	seasonal
sha	soil heat accumulator
sou	soil outside the U-tube
source	source side
TD	fixed temperature difference control strategy
ti	inlet water of the water tank
to	outlet water of the water tank
user	user side

Abbreviations

ACSEU	energy use of auxiliary cooling system
ATRSHA	daily average temperature rise of soil heat accumulator
ATRSHAS	seasonal average temperature rise of soil heat accumulator
ATRSOU	daily average temperature rise of soil outside the U-tube
ATRSOUS	seasonal average temperature rise of soil outside the U-tube
COP	coefficient of performance
CTICR	cooling tower input capacity ratio
FET	fixed entering temperature control strategy
FTD	fixed temperature difference control strategy
FRT	fixed running time control strategy
GHE	ground heat exchanger
GSHP	ground-source heat pump
HGSHP	hybrid ground-source heat pump
PAHD	percentage of daily auxiliary heat dissipation to total daily condensation load
SEU	daily system energy use
SEUS	seasonal system energy use
UEU	daily energy use of heat pump unit
UEUS	seasonal energy use of heat pump unit

1. Introduction

Ground source heat pump (GSHP) as one of the most energy efficient and environmental-friendly air-conditioning technologies, has been receiving increasing attention since it has been developed [1-3]. One of the major challenges relating to the application of GSHP systems is the ground thermal imbalance, which can result in performance deterioration of GSHP systems [4-6].

In order to solve this problem, hybrid ground source heat pump (HGSHP) systems, which utilize auxiliary heat sink or source to supply a fraction of building cooling or heating demand, have been studied [7-9]. The use of HGSHP systems can effectively alleviate ground thermal imbalance, and in the meantime, can reduce the initial costs and ground area requirement in comparison to conventional stand-alone GSHP systems [10, 11]. In cooling dominated areas, where cooling demand is generally higher than heating demand, cooling tower is normally used as the auxiliary heat rejecter in HGSHP systems. Fig. 1 illustrates two different types of cooling tower assisted GSHP systems with serial configuration and parallel configuration.

The feasibility and effectiveness of cooling tower assisted GSHP systems have been extensively studied. Man et al. [5, 12], for instance, investigated the performance of a cooling tower assisted GSHP system in hot climate conditions through simulations. The simulation results showed that this HGSHP system can effectively solve the heat accumulation problem and save both initial cost and operating cost as compared to a conventional GSHP system. Hackel and Pertzborn [13] analyzed the performance of three HGSHP systems including two cooling tower assisted systems and one boiler assisted system by using both the operation data collected from the real projects and simulation data. The results showed that appropriate use of HGSHP systems

115 in buildings with unbalanced cooing and heating loads was more cost effective than that using the
116 stand-alone GSHP or conventional systems. Sayyadi and Nejatolahi [14] performed a
117 multi-objective optimization of a cooling tower assisted GSHP system, in which both
118 thermodynamic and thermoeconomic objectives were considered simultaneously. The major
119 design parameters of this HGSHP system were optimized using a genetic algorithm. Park et al.
120 [15] investigated the performance of a cooling tower assisted GSHP system with different
121 amounts of refrigerant charge, and different secondary fluid flow rates of the ground loop and the
122 supplemental loop, respectively. The optimal refrigerant charge and optimal secondary fluid flow
123 rates were identified through a number of experimental tests. The coefficient of performance
124 (COP) of this HGSHP system with optimal operating parameters was 21% higher than that of a
125 conventional GSHP system. Lee et al. [16] investigated the transient characteristics of a cooling
126 tower assisted GSHP system through experimental tests. The results showed that the performance
127 enhancement of this system was highly dependent on the leaving fluid temperature set-point of
128 the ground heat exchanger (GHE). The COP of this HGSHP system at the optimal set-point
129 temperature of 30 ^{o}C was 7.2% higher than that of a stand-alone GSHP system. Several studies
130 evaluated the performance of the cooling tower assisted GSHP systems with different flow loop
131 configurations. For instance, Park et al. [17] experimentally investigated the energy performance
132 of a cooling tower assisted GSHP system with both parallel and serial configurations, under
133 various leaving fluid temperatures of the GHE and flow rates in the supplemental loop,
134 respectively. The results showed that the COPs of the HGSHP with parallel and serial
135 configurations were 18% and 6%, higher than that of a stand-alone GSHP system, respectively.
136 The HGSHP with parallel configuration rejected more heat into the supplemental plate heat

137 exchanger than that with serial configuration at a lower flow rate in the supplemental loop. Lee et
138 al. [18] also analyzed the performance of a cooling tower assisted GSHP system with parallel and
139 serial configurations through experimental tests. The experimental results indicated that the
140 HGSHP system with serial configuration with up-stream flow showed a relatively higher COP
141 and a lower heat accumulation than that with the downstream flow. The COPs of the HGSHP
142 system with the serial and parallel configurations were 15% and 7% higher than that of a
143 stand-alone GSHP system, respectively. Zhou et al. [19] developed a simulation system for a
144 cooling tower assisted GSHP with parallel and serial configurations in TRNSYS. The 30 years
145 operation of the system under different operation schemes was simulated. The results showed that
146 activating the cooling tower during the transition seasons when the temperature difference
147 between the air wet-bulb temperature and the ground temperature was 8-12 ^{o}C offered the highest
148 benefits of using this HGSHP system. The system with the parallel configuration used less energy
149 in 30 years operation than that with the serial configuration. The results from the aforementioned
150 studies demonstrated that cooling tower assisted GSHP systems outperformed conventional
151 stand-alone GSHP systems in terms of energy use and ground thermal balance maintenance.
152 However, the operating parameters and control strategies used for such systems should be
153 carefully determined.

154 The energy performance of a cooling tower assisted GSHP system highly depends on the
155 control strategies used. The control strategies used for cooling tower assisted GSHP systems
156 could be broadly categorized into three groups: 1) to activate the cooling tower based on the
157 temperature set-point of the heat pump entering/existing fluid; 2) to activate the cooling tower
158 based on the temperature difference between the heat pump entering/exiting fluid temperature

and the ambient air dry-bulb/wet-bulb temperature and; 3) to activate the cooling tower during a fixed time period. The results from several studies [5, 20-22] suggested that the control strategies that have longer operation hours of the cooling tower provided more benefits than those with less operation hours, and the control strategy based on the difference between the heat pump exiting fluid temperature and the air wet-bulb temperature outperformed the others. Yang et al. [23] investigated three intermittent operation strategies for a HGSHP system with a double-cooling tower to solve the problem of the underground heat accumulation. The three operation strategies activated the cooling towers and the GHE at different time periods in a week. The simulation results showed that the intermittent operation strategies investigated can significantly alleviate soil heat accumulation. The optimal intermittent operating condition that favors both power consumption reduction and soil temperature recovery was also identified through an economic analysis. Fan et al. [24] purposed and analyzed four control strategies for cooling tower assisted GSHP systems. The results showed that, the conrol strategy that combined the entering water temperature control and wet-bulb temperature difference control has the lowest energy use, but the soil temperature rise after 10 years of operation was slightly higher than 3°C. The other three strategies with the cooling tower running during the transition season can control the soil temperature rise after 10 years of operation within 3°C but lose the benefit of lower energy use. Hu et al. [25, 26] employed a control strategy using extremum seeking control to optimize the operation of a cooling tower assisted GSHP system. The combined power consumption of the GHE loop water pump, cooling tower fan and pump, and heat pump compressor was minimized through optimizing the cooling tower fan speed and water pump speed. Cui et al. [27] analyzed the performance of system configurations and control strategies of a cooling tower assisted GSHP

system using TRNSYS. It was found that the optimal auxiliary cooling ratio for both parallel and serial configurations of this HGSHP was 0.5. The fixed load ratio control and the fixed entering temperature control can provide a better performance for parallel and serial HGSHP systems, respectively.

The majority of the existing studies on the control of cooling tower assisted GSHP systems focused on the system performance comparison of using different control strategies or the control of the system under a certain cooling tower input capacity. The system performance under varied cooling tower input capacities and the relationship between the control strategy and the optimal cooling tower input capacity have not been extensively studied.

In this study, the performance of a cooling tower assisted GSHP system with serial configuration implemented in an office building was first evaluated. A simulation system was then developed using TRNSYS and validated using the operation data collected from the experiments. The system performance and the soil temperature variation under various cooling tower input capacities and different operation scenarios were then studied through simulation exercises. The optimal cooling tower input capacity under different system operation scenarios for the system was then identified. The method used in this study can be used to guide and facilitate the design and control of cooling towers in cooling tower assisted GSHP systems.

2. Description of the experimental system

The experimental system concerned was implemented in an office building in Ningbo University of Technology, which is located in the hot summer and cold winter region of China. The system was used to provide cooling and heating to the building with the design cooling and heating

capacities of 42.5 kW and 30.0 kW, respectively. The schematic and outlook of the experimental system are illustrated in Fig. 2 and Fig. 3, respectively. The system mainly consists of two water-to-water heat pump units, two chilled water pumps (e.g. one for standby) and two cooling water pumps (e.g. one for standby), ground heat exchangers (GHEs), an indoor air handling system, an auxiliary cooling system, and a monitoring and control system. The specifications of the major components are summarized in Table 1.

In this system, the cooling water at the source side of the HGSHP system is circulated among the condenser of the heat pump, the auxiliary cooling system and the GHE loop, while the chilled water at the load side is circulated between the evaporator of the heat pump and the indoor air handling system. The ground heat exchanger (GHE) loop was sized based on the design heating load and the measured soil properties using the design method presented in [10, 28]. The borehole field consists of 12 single U-tube heat exchanger boreholes with a depth of 75 meters each. The layout of the borehole field is shown in Fig. 4 and the major design parameters of the GHEs are summarized in Table 2. Fan coils were used for indoor air handling. The auxiliary cooling system was sized based on the difference between the building design cooling and heating loads using the peak algorithm method developed by Kavanaugh and Rafferty [29], which is the recommended method to size the auxiliary cooling system of HGSHP systems in Chinese standard [30]. The water tank in the auxiliary cooling system was used as a heat exchanger between the auxiliary cold source and the cooling water circulation. The auxiliary cold source used in the system is city water. The measuring points above the ground and underground are shown in Fig. 2 and Fig. 4, respectively. The measuring points above the ground were used to measure the water temperature, flow rates at different locations and power consumption, while

225 the measuring points under the underground were used to measure the borehole wall temperatures
226 at the depths of 15 m, 25 m, 35 m, 45 m, 55 m, 65 m and 75 m of each borehole, respectively.
227 The details of the measuring equipment are summarized in Table 3.
228 The auxiliary cooling system was connected with the GHEs in series with the up-stream flow
229 configuration, in which the cooling water flows through the condenser, the auxiliary system and
230 the GHEs in series, since the system with the up-stream flow configuration can result in a better
231 energy performance than that with the down-stream flow configuration [18]. This experimental
232 system can operate with or without the auxiliary cooling system through ON/OFF control of three
233 isolation valves (valves V1-V3 in Fig. 2). When the system operates without the auxiliary cooling
234 system (i.e. by opening the valve V1 and closing the valves V2 and V3), the heat will be fully
235 rejected to the ground through the GHEs. When the system operates with the auxiliary cooling
236 system (by opening the valves V2 and V3 and closing the valve V1), a fraction of heat will be
237 dissipated through the auxiliary cooling system, which is controlled by changing the water side
238 flow rate of the auxiliary cooling system through regulating the valves V3 and V4.
239
240 **3. Modelling of the cooling tower assisted GSHP system**
241 A virtual simulation system of the cooling tower assisted GSHP system was developed based on
242 the experimental system using TRNSYS. In this virtual system, a cooling tower with the same
243 capacity as that of the auxiliary cooling system in the experimental system was used as the
244 auxiliary heat rejecter. The major design parameters of the cooling tower are listed in Table 4. A
245 plate heat exchanger was used between the cooling tower circulation and the cooling water
246 circulation instead of a water tank. The GSHP system was simplified with one heat pump unit

247 with the same heating and cooling capacity as the sum of the two heat pump units used in the
248 experimental system. The other components used in this virtual system and their parameters were
249 the same as that used in the experimental system.
250 An illustration of the virtual simulation system is shown in Fig. 5. There are three major water
251 loops in this system, including the chilled water loop, the cooling water loop and the auxiliary
252 cooling loop. The major simulation models used to develop the simulation system are described
253 below.

254 **3.1 Water-to-water heat pump model**

255 The performance of the water-to-water heat pump was simulated using the model presented in
256 ASHRAE Handbook [31]. In this model, the instantaneous power consumption of the heat pump
257 is represented as a function of the chilled water inlet temperature and cooling water inlet
258 temperature of the heat pump, as expressed in Eq. (1).

259 $$w_{HP,a} = w_{HP,r} \sum_{i=0}^{2} \sum_{j=0}^{2} D_{ij} (T_{user,in,r} - T_{user,in,r})^{i} (T_{source,in,a} - T_{source,in,r})^{j} \quad (1)$$

260 where w is the power consumption, T is the temperature and D_{ij} are the regression coefficients,
261 which were determined based on the performance data provided by the manufacturer, and the
262 values used are provided in Table 5. The subscripts *HP, a, r, user* and *in* represent heat pump,
263 actual condition, rated condition, user side and inlet, respectively.

264 **3.2 Ground heat exchanger model**

265 The duct storage (DST) system model proposed by Hellstrom [32] was used to simulate the
266 performance of vertical GHEs. This model was developed based on the finite line-source model
267 and has been successfully included in TRNSYS as a standard model (Type 557). The detailed

268 structure of the DST model is shown in Fig. 6. In this model, the whole borehole field was
269 modelling as one heat accumulator instead of simulation of each individual borehole.

270 **3.3 Cooling tower model**

271 Cooling tower is used as the auxiliary heat rejecter in this HGSHP system. The standard cooling
272 tower model (Type 51a) in the TRNSYS library was used to simulate the performance of the
273 counter flow cooling tower, in which the heat transfer process was simulated using ε - NTU
274 method proposed by Jaber and Webb [33]. The schematic of the counter flow cooling tower used
275 in the system is shown in Fig. 7.

276 **3.4 Plate heat exchanger model**

277 In this study, the plate heat exchanger was used between the auxiliary cooling loop and the
278 cooling water loop. The simplified heat exchanger model with a constant heat transfer efficiency
279 of 0.8 between the primary and secondary side fluid was used in the simulation.

280 **3.5 Water pump model**

281 The chilled water pump and cooling water pump used in this HGSHP system are constant speed
282 water pumps and their power consumption was calculated by using Eq. (2).

283 $$w_p = \frac{\rho g G_a H}{\eta_p} \tag{2}$$

284 where, ρ is the density of the working fluid, g is the gravity acceleration, G is the water flow
285 rate, H is the pump head, η is the efficiency, and the subscripts a and p represent actual
286 condition and pump, respectively.

287 The auxiliary loop circulation pump used was a variable speed pump, which was used to
288 control the cooling tower input capacity by varying the water side flow rate of the cooling tower.

A flow rate control signal was used, which was set as the proportion of the desired water flow rate to the design water flow rate of the cooling tower. This flow rate control signal associated with a number of control logics and signals (i.e. operating time, temperature, temperature difference, etc.) formed the control logic for the variable speed pump. For a certain simulation scenario, this pump control logic was firstly determined, and it remained constant during the simulation. The power consumption of the variable speed pump can be calculated using Eq. (8) [34].

$$w_p = \frac{\rho g G_a^{\ 3} H_r}{\eta_p G_r^{\ 2}} \tag{3}$$

4. Operation scenarios for cooling tower assisted GSHP systems

There are three typical operation schedules of the building air-conditioning system in different types of office buildings. The typical operation schedules for the research and higher education institutions, normal office buildings and government office buildings and primary and secondary schools are from 6:00 to 22:00, from 8:00 to 18:00, and from 8:30 to 17:30, respectively. There are also three typical control strategies that are used to operate the cooling tower assisted GSHP system and they are presented as follows [20, 35].

(1) Control strategy based on the fixed entering cooling water temperature (FET): the cooling tower is activated when the entering cooling water temperature of the heat pump unit exceeds a pre-determined temperature;

(2) Control strategy based on the fixed temperature difference (FTD): the cooling tower is activated when the difference between the cooling water leaving temperature of the heat pump unit and the dry-bulb (or wet-bulb) temperature of ambient air exceeds a certain

value;

(3) Control strategy based on the fixed running time (FRT): the cooling tower is activated during a predetermined time period of a day.

In this study, nine operation scenarios with different operation schedules and control strategies were considered. The daily and seasonal performance of this cooling tower assisted GSHP system under these nine operation scenarios were investigated using the simulation system developed. The daily performance investigation was carried out in a typical summer day, and the seasonal performance investigation was carried out during the whole cooling season from 20th June to 10th September. The details of these operation scenarios are provided in Table 6, in which the set-points of each control strategy were determined based on the building load characteristic, local standards and relevant studies [20, 23, 27, 35]. In the FET control strategy, the temperature set-point was set at 32 ^{o}C. In the FTD control strategy, the cooling tower was activated when the difference between the leaving cooling water temperature of the heat pump unit and the wet-bulb temperature of ambient air was larger than 2.0 ^{o}C, and was deactivated when the temperature difference was less than 1.5 ^{o}C. In the FRT control strategy, the cooling tower was activated during the whole operation period. The FET control and FTD control were realized by using a temperature difference controller (Type 2) in TRNSYS and the FRT control strategy was simply realized by setting the operation period of the GSHP system and the auxiliary cooling system.

5. Results and discussion

5.1 Experimental tests

The experimental tests were carried out in July and August in 2016. During the tests, the

HGSHP system was operated based on the working hours and the cooling demand of the office building. The system was generally operated from 8:30 to 17:30 in working days, but the operation duration can be extended manually to adapt to the research requirement. The two heat pump units were sequenced based on their design cooling capacities and the building load.

The variation in the measured daily borehole wall temperature, the calculated daily accumulated heat dissipations of the GHEs and auxiliary cooling system, and the daily accumulated system power consumption were used to validate the simulation system. The average of all the measured underground temperatures was considered as the borehole wall temperature. The daily accumulated heat dissipation of the GHEs and the auxiliary cooling system were calculated using Eqs. (4) and (5), respectively, in which the transient heat exchanges of the GHEs and the auxiliary cooling system were calculated by using Eqs. (6) and (7), respectively. The daily accumulated power consumption was calculated using Eq. (8). The percentage of the daily auxiliary heat dissipation to the total daily condensation load (PAHD) can be determined using Eq. (9), based on the calculation results from Eqs. (4)-(7). The total daily condensation load was the sum of the daily accumulated heat dissipation of the GHEs and the auxiliary cooling system.

$$Q_g = \sum_{i=1}^{n} (\dot{Q}_g \cdot \Delta t_i) \tag{4}$$

$$Q_{aux} = \sum_{i=1}^{n} (\dot{Q}_{aux} \cdot \Delta t_i) \tag{5}$$

$$\dot{Q}_g = \rho G_c C (T_{gi} - T_{go}) \tag{6}$$

$$\dot{Q}_{aux} = \rho G_c C (T_{ti} - T_{to}) \tag{7}$$

$$W = \sum_{i=1}^{n} (w \cdot \Delta t_i) \tag{8}$$

$$PAHD = \frac{Q_{aux}}{Q_g + Q_{aux}} \times 100\% \quad (9)$$

where, Q is the daily accumulated heat dissipation, $\dot{Q}$ is the transient heat dissipation, Δt_i is the measuring time interval, n is the total number of measuring time intervals in a day, G is the water flow rate, C is the specific heat capacity of the working fluid, W is the daily accumulated power consumption, and the subscripts *g, aux, c, gi, go, ti* and *to* represent GHE, auxiliary cooling system, cooling water, inlet water of the GHE, outlet water of the GHE, inlet water of the water tank and outlet water of the water tank, respectively.

5.2 Model validation result

The simulation model of the cooling tower assisted GSHP system was validated using the system performance data collected from the experimental tests in two typical summer days (i.e. 28th July and 13th August) in 2016. In order to get enough performance data for model validation, the system operation duration on 28th July was extended manually from 7:42 to 19:02, during which the system operated without the auxiliary cooling system. The system operation duration on 13th August was from 8:44 to 18:00, during which the system operated with the auxiliary cooling system. The system operation duration, the PAHD, the initial borehole wall temperature and the system control strategy used in the simulation were the same as those of the experimental system. The validation results when the system operated with and without auxiliary cooling system are presented in Fig. 8 and Fig. 9, respectively. It can be observed that the accumulated heat pump and system power consumption, the borehole wall temperature (T_b) and the instantaneous COPs of the heat pump and the system obtained from the simulation agreed well with those determined based on the experimental data during the majority of the operation period

375 in both two days. The simulated T_b normally decreased a little bit at the beginning of the
376 simulation mainly due to the characteristic of the DST model and the iterative algorithm used in
377 the model to calculate the soil temperature, and it was then gradually increased.

378 The simulated and measured borehole wall temperatures, the daily average borehole wall
379 temperatures during the system operation, the daily accumulated power consumption of the heat
380 pump unit and the whole system as well as the daily average COPs of the heat pump unit and the
381 whole system when the system operated with or without auxiliary cooling system were
382 summarized in Table 7. It can be seen that the daily soil temperature variation, the daily
383 accumulated power consumption and the daily average COPs obtained from the simulation
384 agreed well with those obtained from the experimental tests. The highest relative error between
385 the simulation and the experiments was less than 3.4%, indicating the effectiveness of the system
386 simulation model used. It is worthwhile to note that, the system operated with the auxiliary
387 cooling system achieved a higher daily average COP of the whole system and a lower
388 temperature rise in the borehole wall, in comparison to the system operated without the auxiliary
389 cooling system.

390 **5.3 Auxiliary heat dissipation of the cooling tower under different operation scenarios**

391 Fig. 10 presents the relationship between the PAHD and the cooling tower input capacity ratio
392 (CTICR) under different system operation scenarios in the typical summer day. CTICR was
393 defined as the ratio of the cooling tower input capacity to the maximum capacity of the cooling
394 tower. The cooling tower input capacity referred to the cooling tower capacity under the actual
395 water flow rate in the auxiliary cooling loop, while the maximum capacity of the cooling tower
396 referred to the cooling tower capacity under the design water flow rate in the auxiliary cooling

loop. Therefore, CTICR can be expressed in Eq. (10).

$$\mathrm{CTICR}=\beta\frac{G_{aux,a}}{G_{aux,des}} \tag{10}$$

where, β is the correction coefficient determined based on the performance data provided by the manufacturer, and the subscripts *aux* and *des* reparent auxiliary cooling system and design, respectively.

It can be seen that, under the FTD control and FRT control, the PAHD increased with the increase of the CTICR, but the increasing rate was gradually decreased. The highest PAHD of 60% was achieved when the CTICR reached 100%. Under the FET control, the PAHD increased with the increase of the CTICR when CTICR was less than 54%, but it decreased when further increasing CTICR. This is mainly because, under the FET control, the cooling tower was only activated when the entering cooling water temperature of the heat pump unit exceeded 32 ^{o}C. Increasing CTICR boosted the heat dissipation capacity of the cooling tower but reduced the operation duration of the cooling tower. Further increasing CTICR resulted in a decrease in the total auxiliary heat dissipation. The relationship between PAHD and CTICR revealed that increasing the cooling tower input capacity did not result in an equivalent increase in the auxiliary heat dissipation. The optimal CTICR should be determined based on the actual operation condition and the control strategy used.

5.4 Influence of the cooling tower input capacity on the soil temperature

Under the cooling working condition, the heat rejection to the ground will increase the ground temperature around the GHEs. The rise in the ground temperature will gradually deteriorate the cooling performance of GSHP systems. The main purpose of using the auxiliary cooling system

418 in a GSHP system is to achieve annual ground thermal balance, preventing performance
419 deterioration. Therefore, the influence of the cooling tower input capacity on the soil temperature
420 was investigated.

421 In this study, the performance of the 12 boreholes were assumed to be identical, since they
422 were used simultaneously during the system operation with the same inlet water temperature and
423 fluid flow rate. The average temperature of the soil heat accumulator and the average soil
424 temperature outside the U-tube were simulated using the DST model.

425 Fig. 11 presents the average temperature rise of the soil heat accumulator (ATRSHA) and the
426 average temperature rise of the soil outside the U-tube (ATRSOU) at the end of different
427 operation hours, and they were determined using Eq. (11) and Eq. (12), respectively.

428 $$\mathrm{ATRSHA}= (T_{sha,d,i} - T_{sha,d,e}) \quad (11)$$

429 $$\mathrm{ATRSOU}= (T_{sou,d,i} - T_{sou,d,e}) \quad (12)$$

430 where, the subscripts *sha, sou, d, i and e* represent soil heat accumulator, soil outside the U-tube,
431 daily, initial and end, respectively.

432 It can be observed that the use of cooling tower was able to alleviate the soil heat
433 accumulation. Both ATRSHA and ATRSOU reduced significantly with the increase of CTICR
434 when it was less than 50%, while this reduction became less significant when further increasing
435 CTICR. ATRSHA and ATRSOU can be reduced up to 0.5 ^{o}C and 3.2 ^{o}C respectively when the
436 capacity of the cooling tower was fully used (i.e. 100% CTICR). It can also be seen that the FRT
437 control was the most effective strategy to alleviate the soil heat accumulation, followed by the
438 FTD control, and the FET control.

439 Fig. 12 presents the seasonal average temperature rise of the soil heat accumulator

(ATRSHAS) and the seasonal average temperature rise of the soil outside the U-tube (ATRSOUS) after the whole cooling season under different operation scenarios, and they were calculated using Eq. (13) and Eq. (14), respectively.

$$\text{ATRSHAS} = (T_{sha,s,i} - T_{sha,s,e}) \quad (13)$$

$$\text{ATRSOUS} = (T_{sou,s,i} - T_{sou,s,e}) \quad (14)$$

where, the subscripts *s* represents seasonal.

It can be observed that the curves of ATRSHAS and ATRSOUS shared the similar variation trend as those of ATRSHA and ATRSOU, respectively. Both ATRSHAS and ATRSOUS can be reduced significantly when the cooling tower was used. The ATRSHAS under all operation scenarios was less than 2.0 ^{o}C when the CTICR was greater than 50%, which was the acceptable temperature rise after the cooling season operation based on the annual simulation results.

The above results indicated that the input cooling tower capacity in the HGSHP system should not be less than 50% of its maximum cooing capacity during the operation in order to effectively alleviate the soil heat accumulation and maintain the ground thermal balance.

5.5 Influence of the cooling tower input capacity on the system energy use

Fig. 13 shows the daily system energy use (SEU) and the daily heat pump unit energy use (UEU) with various CTICRs and under different system operation scenarios. It can be observed that both SEU and UEU were closely related to the CTICR. With the increase of the CTICR, the differences in SEU and UEU among the three control strategies became more significant under all operation schedules.

Under the FRT control and FTD control, UEU always decreased with the increase of CTICR, and the UEU under the FRT control was slightly lower than that under the FTD control. The UEU

462 under the FET control was higher than that under the other control strategies, especially when the
463 CTICR was greater than 50%. Since the actual auxiliary heat dissipation under the FET control
464 was significantly lower than that under the other two control strategies (See Fig. 10), the heat
465 pump unit under the FET control therefore provided more cooling energy, resulting in an increase
466 in the UEU.

467 From Fig. 13, it can also be observed that the CTICR that led to the minimization of SEU was
468 around 63% under all operation scenarios, except for the operation scenario FET8 which was
469 around 44%. Under all operation schedules, the SEU under the FTD control was generally the
470 lowest, and those under the FRT control and FTD control were relatively close to each other.

471 The daily energy use of the auxiliary cooling system (ACSEU) was related to the CTICR and
472 the operation duration of the cooling tower. The relationship between ACSEU and CTICR under
473 the three operation schedules is shown in Fig. 14. It can be observed that the ACSEU under the
474 FTD control was generally lower than that under the FRT control but was higher than that under
475 the FET control.

476 From the above analysis, it can be concluded that under the FRT control, the operating time of
477 the cooling tower was the longest, which resulted in the highest ACSEU and the lowest UEU.
478 However, under the FET control, the operating time of the cooling tower was the lowest, with the
479 lowest ACSEU and the highest UEU. The daily system energy use under both two control
480 strategies were nearly the same. The system under the FTD control consumed the lowest amount
481 of energy in the typical summer day.

482 Fig. 15 shows the seasonal system energy use (SEUS) and the seasonal heat pump unit energy
483 use (UEUS) with the variation of the CTICR under different system operation scenarios. It can be

observed that UEUS decreased with the increase of the CTICR under all operation scenarios. However, the decreasing rate was gradually reduced. Similar to the variation of SEU, there existed an optimal CTICR that minimized the SEUS. This optimal CTICR was around 54% under the operation scenarios FTD16 and FRT16, and was around 63% under the other operation scenarios. The CTICR that minimized the SEUS under all operation scenarios was greater than 50%, which demonstrated that using the optimal CTICR identified could effectively alleviate the soil heat accumulation and minimize the energy use of this HGSHP system. The corresponding cooling tower input capacity under each operation scenario was therefore considered as the optimal cooling tower input capacity. It is worthwhile to note that the optimal cooling tower input capacities identified under all operation scenarios were always less than the maximum capacity of the cooling tower, indicating that the cooling tower determined using the peak algorithm method was oversized. The cooling tower for this HGSHP system could be re-sized based on the optimal cooling tower input capacity identified in this section.

It can also be observed that the SEUS under the FET control was always the highest among the three control strategies. The SEUS under the FRT control was slightly higher than that under the FTD control under all operation scenarios. The FTD control was therefore considered as the optimal control strategy among the three control strategies for this cooling tower assisted GSHP system. It is worthwhile to note that these results were highly dependent on the climate condition, and the optimal input cooling tower capacity and the optimal control strategy could be different under different climate conditions.

6. Conclusion

In this paper, the optimal cooling tower input capacity of a cooling tower assisted ground source heat pump (GSHP) system was investigated based on experiments and simulations. An experimental system of a hybrid GSHP (HGSHP) system with serial configuration was first developed and implemented in a real engineering condition in the hot summer and cold winter region of China. A simulation model of the cooling tower assisted GSHP system was then developed based on this experimental system using TRNSYS and was validated using the operation data collected from the experimental system. The system performance and soil temperature variation under different cooling tower capacity ratios (CTICRs) and different operation scenarios was investigated through simulation exercises. The model validation results showed that, the majority of the operating parameters obtained from the simulation agreed well with those determined from the experimental tests. The simulation results showed that the soil heat accumulation could be effectively alleviated when the CTICR was greater than 50%. The optimal cooling tower input capacity was highly dependent on the system operation scenario used. The longest operating time of the cooling tower was required under the fixed running time (FRT) control and the lowest operating time of the cooling tower was required under the fixed entering cooling water temperature (FET) control. The system energy use under the two control strategies were nearly the same, both higher than that under the fixed temperature difference (FTD) control. The optimal CTICR was around 54% under the operation scenarios that operated the system from 6:00 to 22:00 under the FRT control, and operated the system from 6:00 to 22:00 under the FTD control, while that under other operation scenarios was around 63%. The optimal control strategy identified was the FTD control, under which the system consumed the least amount of energy

527 throughout the whole cooling season. The method used in this study can be used to guide and
528 facilitate the optimal design and control of cooling towers in cooling tower assisted GSHP
529 systems.
530
531 **References**
532 [1] L. Pu, D. Qi, K. Li, H. Tan, Y. Li, Simulation study on the thermal performance of vertical
533 U-tube heat exchangers for ground source heat pump system, Applied Thermal Engineering, 79
534 (2015) 202-213.
535 [2] Z. Wang, F. Wang, J. Liu, Z. Ma, E. Han, M. Song, Field test and numerical investigation on
536 the heat transfer characteristics and optimal design of the heat exchangers of a deep borehole
537 ground source heat pump system, Energy Conversion and Management, 153 (2017) 603-615.
538 [3] S. Huang, Z. Ma, P. Cooper, Optimal design of vertical ground heat exchangers by using
539 entropy generation minimization method and genetic algorithms, Energy Conversion and
540 Management, 87 (2014) 128-137.
541 [4] Y. Yu, Z. Ma, X. Li, A new integrated system with cooling storage in soil and ground-coupled
542 heat pump, Applied Thermal Engineering, 28 (11-12) (2008) 1450-1462.
543 [5] Y. Man, H. Yang, J. Wang, Study on hybrid ground-coupled heat pump system for
544 air-conditioning in hot-weather areas like Hong Kong, Applied Energy, 87 (9) (2010) 2826-2833.
545 [6] Z. Wang, F. Wang, Z. Ma, X. Wang, X. Wu, Research of heat and moisture transfer influence
546 on the characteristics of the ground heat pump exchangers in unsaturated soil, Energy and
547 Buildings, 130 (2016) 140-149.
548 [7] G. Phetteplace, W. Sullivan, Performance of a hybrid ground-coupled pump system, ASHRAE

549 transactions, 104 (1998) 763.
550 [8] A.D. Chiasson, C. Yavuzturk, Assessment of the viability of hybrid geothermal heat pump
551 systems with solar thermal collectors, ASHRAE transactions, 109 (2) (2003) 487-500.
552 [9] Y. Man, H. Yang, J.D. Spitler, Z. Fang, Feasibility study on novel hybrid ground coupled heat
553 pump system with nocturnal cooling radiator for cooling load dominated buildings, Applied
554 Energy, 88 (11) (2011) 4160-4171.
555 [10] ASHRAE, Commercial/institutional ground-source heat pump engineering manual,
556 ASHRAE, Inc., Atlanta, 1995.
557 [11] Z.S. Qi, Q. Gao, Y. Liu, Y.Y. Yan, J.D. Spitler, Status and development of hybrid energy
558 systems from hybrid ground source heat pump in China and other countries, Renewable and
559 Sustainable Energy Reviews, 29 (2014) 37-51.
560 [12] M. Yi, Y. Hongxing, F. Zhaohong, Study on hybrid ground-coupled heat pump systems,
561 Energy and Buildings, 40 (11) (2008) 2028-2036.
562 [13] S. Hackel, A. Pertzborn, Effective design and operation of hybrid ground-source heat pumps:
563 three case studies, Energy and Buildings, 43 (12) (2011) 3497-3504.
564 [14] H. Sayyadi, M. Nejatolahi, Thermodynamic and thermoeconomic optimization of a cooling
565 tower-assisted ground source heat pump, Geothermics, 40 (3) (2011) 221-232.
566 [15] H. Park, J.S. Lee, W. Kim, Y. Kim, Performance optimization of a hybrid ground source heat
567 pump with the parallel configuration of a ground heat exchanger and a supplemental heat rejecter
568 in the cooling mode, International Journal of Refrigeration, 35 (6) (2012) 1537-1546.
569 [16] J.S. Lee, H. Park, Y. Kim, Transient performance characteristics of a hybrid ground-source
570 heat pump in the cooling mode, Applied Energy, 123 (2014) 121-128.

571 [17] H. Park, J.S. Lee, W. Kim, Y. Kim, The cooling seasonal performance factor of a hybrid
572 ground-source heat pump with parallel and serial configurations, Applied Energy, 102 (2013)
573 877-884.
574 [18] J.S. Lee, K.S. Song, J.H. Ahn, Y. Kim, Comparison on the transient cooling performances of
575 hybrid ground-source heat pumps with various flow loop configurations, Energy, 82 (2015)
576 678-685.
577 [19] S. Zhou, W. Cui, Z. Li, X. Liu, Feasibility study on two schemes for alleviating the
578 underground heat accumulation of the ground source heat pump, Sustainable Cities and Society,
579 24 (2016) 1-9.
580 [20] C. Yavuzturk, J.D. Spitler, Comparative study of operating and control strategies for hybrid
581 ground-source heat pump systems using a short time step simulation model, ASHRAE
582 transactions, 106 (2000) 192-209.
583 [21] Q. Zhang, N. Lv, S. Chen, H. Shi, Z. Chen, Study on operating and control strategies for
584 hybrid ground source heat pump system, Procedia Engineering, 121 (2015) 1894-1901.
585 [22] Z. Sagia, C. Rakopoulos, New control strategy for a hybrid ground source heat pump system
586 coupled to a closed circuit cooling tower, Journal of Applied Mechanical Engineering, 1 (2)
587 (2012) 1-8.
588 [23] J. Yang, L. Xu, P. Hu, N. Zhu, X. Chen, Study on intermittent operation strategies of a hybrid
589 ground-source heat pump system with double-cooling towers for hotel buildings, Energy and
590 Buildings, 76 (2014) 506-512.
591 [24] R. Fan, Y. Gao, L. Hua, X. Deng, J. Shi, Thermal performance and operation strategy
592 optimization for a practical hybrid ground-source heat-pump system, Energy and Buildings, 78

593 (2014) 238-247.
594 [25] B. Hu, Y. Li, B. Mu, S. Wang, J.E. Seem, F. Cao, Extremum seeking control of hybrid
595 ground source heat pump system, International Refrigeration and Air Conditioning Conference,
596 2014.
597 [26] B. Hu, Y. Li, B. Mu, S. Wang, J.E. Seem, F. Cao, Extremum seeking control for efficient
598 operation of hybrid ground source heat pump system, Renewable Energy, 86 (2016) 332-346.
599 [27] W. Cui, S. Zhou, X. Liu, Optimization of design and operation parameters for hybrid
600 ground-source heat pump assisted with cooling tower, Energy and Buildings, 99 (2015) 253-262.
601 [28] Standard China, Technical Guidelines for Building Application of Ground Source Heat
602 Pump System in Ningbo (S10-2010), Ministry of Housing, Urban and Rural Development of
603 China, China, 2010.
604 [29] S.P. Kavanaugh, K.D. Rafferty, Ground-source heat pumps: design of geothermal systems
605 for commercial and institutional buildings, American Society of Heating, Refrigerating and
606 Air-Conditioning Engineers, 1997.
607 [30] Standard China, Technical code for ground-source heat pump system (GB50366-2009),
608 Ministry of Housing, Urban and Rural Development of China, China, 2009.
609 [31] Systems and equipment, American Society of Heating, Refrigerating, and Air Conditioning
610 Engineers, Atlanta, GA, 1992.
611 [32] G. Hellström, Ground heat storage: thermal analyses of duct storage systems, Department of
612 Mathematical Physics, Lund University, Sweden, 1991.
613 [33] H. Jaber, R. Webb, Design of cooling towers by the effectiveness-NTU method, Journal of
614 Heat Transfer, 111 (4) (1989) 837-843.

615 [34] S. Yang, H. Li, J. Yin, Development and application of variable frequency pump module
616 based on TRNSYS, Journal of HV&AC, 8 (2015) 36-41.
617 [35] Y. Ma, Analysis on control strategy in compound gound-source heat pump system of the
618 office building of the typical climate zone, Master's thesis, Chongqing University, 2012.
619

620

621 Table 1 Specifications of the major components used in the experimental system

Component	Number	Parameter
Heat pump unit 1#	1	Rated cooling capacity: 24 kW; Cooling power consumption: 7.3 kW; Rated heating capacity: 26 kW; Heating power consumption: 8.6 kW.
Heat pump unit 2#	1	Rated cooling capacity: 18.5 kW; Cooling power consumption: 3.9 kW; Rated heating capacity: 20.5 kW; Heating power consumption: 5.4 kW.
Load side water pump	2	Rated power: 2 kW; Rated flow rate: 4.5 m^3/h.
Hot water tank	1	Volume: 200 L
Source side water pump	2	Rated power: 2 kW; Rated flow rate: 5.5 m^3/h.
Indoor fan coil	9	Rated cooling capacity: 6.2 kW; Air side flow rate: 1360 m^3/h.

622

623 Table 2 Design parameters of the GHEs

Parameters	Value
Soil thermal conductivity (W/m.K)	1.52
Soil thermal diffusivity (m^2/s)	0.568
Initial soil temperature (^{o}C)	23.1
Borehole depth (m)	75
Number of borehole	12
Borehole distance (m)	4
Borehole radius (m)	0.055
U-tube outer radius (m)	0.0125
U-tube thermal conductivity (W/m.K)	0.42

624

625 Table 3 Details of the major measuring equipment

Name	Measuring parameter	Test range	Accuracy and uncertainty
T type thermocouple	Ambient air temperature	-30~60□	±0.5□
Water proof temperature sensor	Heat pump supply and return chilled water temperatures; User side supply and return water temperatures; Cooling water temperatures before and after heat pump units, auxiliary cooling system and GHEs	-50~+100□	±0.1□
PT 100 water proof temperature sensor	Borehole wall temperature at different depths.	-50~+100□	±0.01□
Flow meter	Flow rates of chilled water and cooling water	0~120□, 0.028~205258 m^3/h	±0.2% f.s or ±1% rdg
Power meter	Power consumption of heat pump	0~15 kW	±0.1% rdg

units and water pumps

626

627 Table 4 Major design parameters of the cooling tower in the virtual HGSHP system

Rated cooling capacity (kW)	Water side flow rate (m^3/h)	Air side flow rate (m^3/h)	Fan power (kW)	Fan diameter (mm)	Tower height (mm)	Sump height (mm)	Sump diameter (mm)
26.0	8	4200	0.18	550	1460	420	930

628

629 Table 5 Regression coefficients of the water-to-water heat pump model

D_{ij}	$i=0$	$i=1$	$i=2$
$j=0$	1.005	0. 012	0.037
$j=1$	0.281	-0.056	0.053
$j=2$	0. 056	0.031	-0.037

630

631 Table 6 System operation scenarios considered in this study

Scenario	Abbreviation	Control strategy	Operation schedule
1	FET16	FET control	6:00-22:00 (16 hours operation)
2	FTD16	FTD control	
3	FRT16	FRT control	
4	FET9	FET control	8:00-17:00 (9 hours operation)
5	FTD9	FTD control	
6	FRT9	FRT control	
7	FET8	FET control	8:30-16:30 (8 hours operation)
8	FTD8	FTD control	
9	FRT8	FRT control	

632

633 Table 7 Comparison of major operation parameters between the experiment and the simulation

Parameter	Without auxiliary cooling system				With auxiliary cooling system			
	Experiment	Simulation	Relative error	Experimental uncertainty	Experiment	Simulation	Relative error	Experimental uncertainty
Operation duration	7:42-19:02	7:42-19:02	0.00%	0.00%	8:44-17:54	8:44-17:54	0.00%	0.00%
PAHD	0	0	-	-	9.10%	9.10%	0.10%	±5.4%
Initial borehole wall temperature (^{o}C)	24.0	24.0	0.00%	±0.5%	23.5	23.5	0.00%	±0.5%
Borehole wall temperature after the system operation (^{o}C)	27.2	27.2	-0.30%	±0.54%	26.0	26.2	0.60%	±0.54%
Daily average borehole wall temperature (^{o}C)	26.5	26.1	-1.20%	±0.54%	25.3	25.3	-0.02%	±0.54%

Power consumption of the heat pump unit (kWh)	68.3	67.9	-0.60%	±1.1%	41.1	41.5	1.00%	±1.1%
Power consumption of the whole system (kWh)	102.4	102.2	-0.2%	±2.1%	68.1	66.5	-2.40%	±2.1%
Daily average COP of heat pump unit	4.62	4.55	-1.5%	±3.3%	5.28	5.10	-3.4%	±3.3%
Daily average COP of the system	2.88	2.83	-1.7%	±5.1%	3.29	3.18	-3.3%	±5.1%

634

635

636 **Figure Captions**

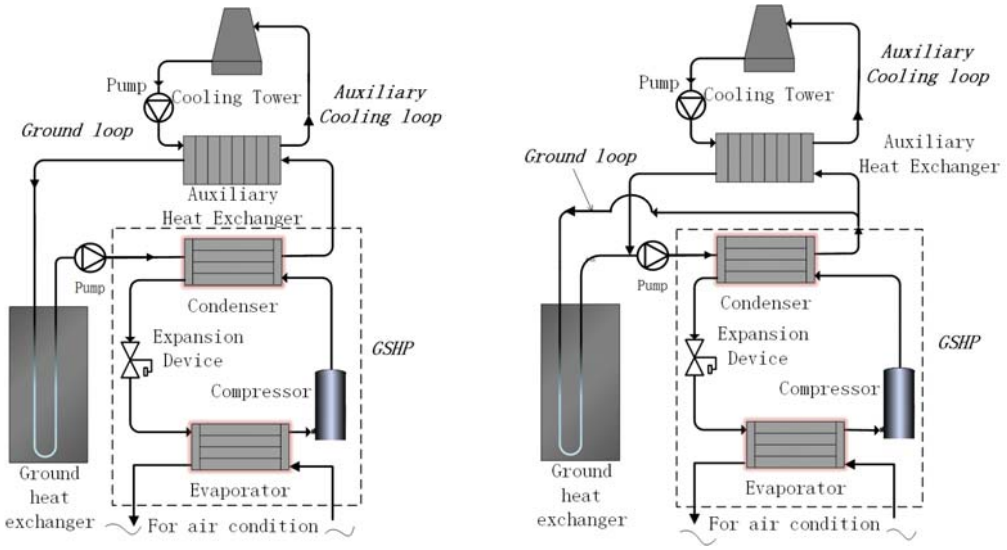

652

653 a) HGSHP with serial configuration b) HGSHP with parallel configuration

654 Fig. 1 Schematic of the cooling tower assisted GSHP systems.

655

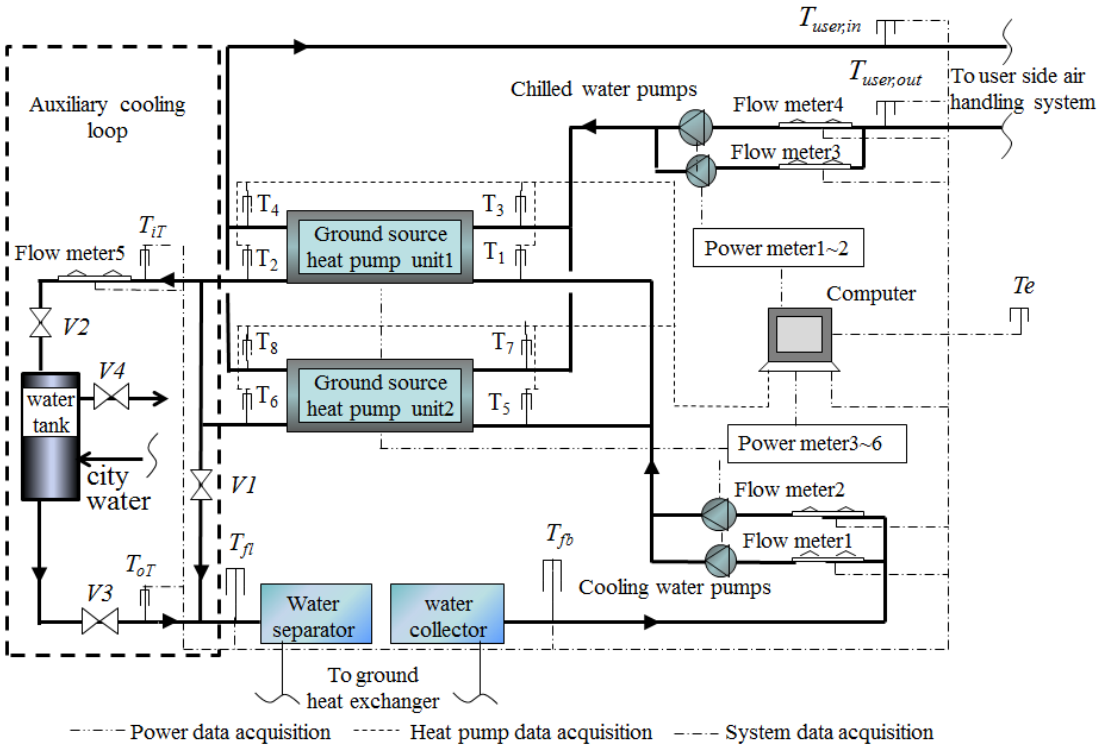

656

657 Fig. 2 Schematic of the experimental system and the measurement points above the ground.

658

Fig. 3 Outlook of the experimental system.

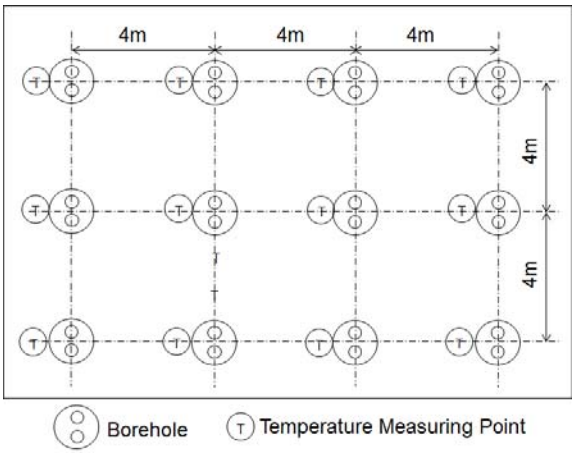

Fig. 4 Layout of the borehole field and the measurement points underground.

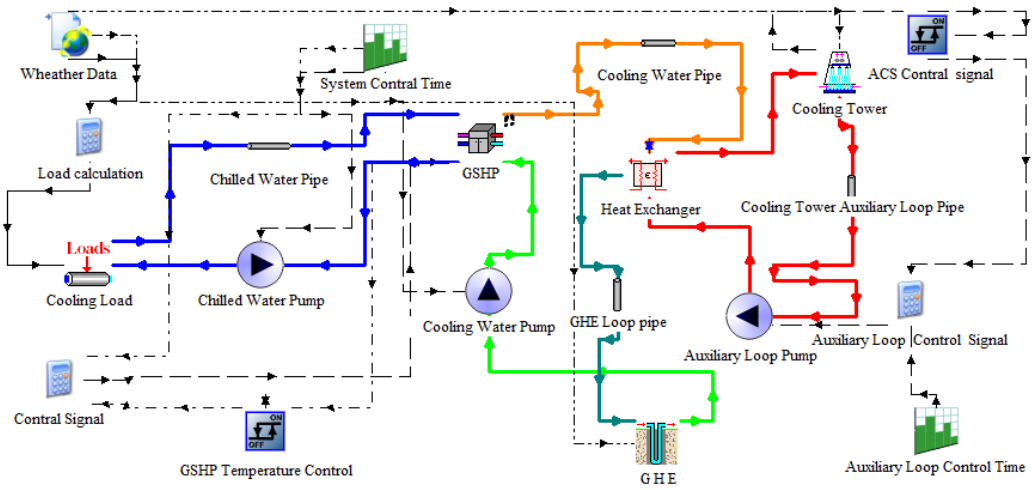

Fig. 5 Illustration of the virtual simulation system developed using TRNSYS.

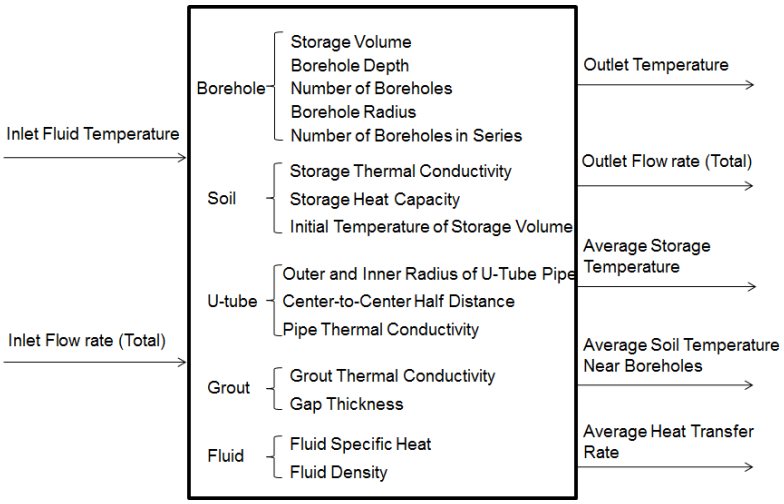

Fig. 6 Structure of the DST model.

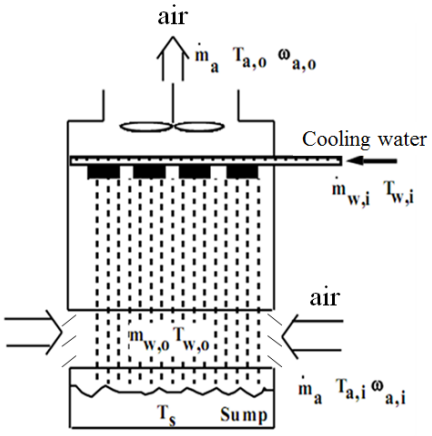

Fig. 7 Schematic of the counter flow cooling tower model.

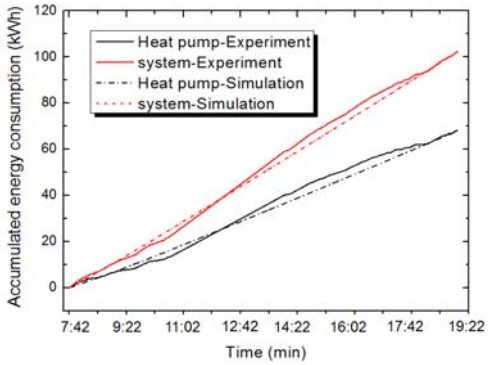

674

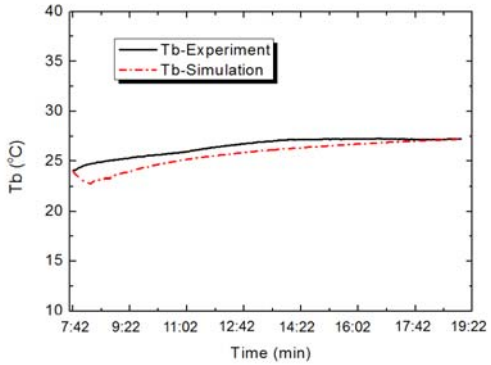

675 a) Accumulated power consumption b) Borehole wall temperature

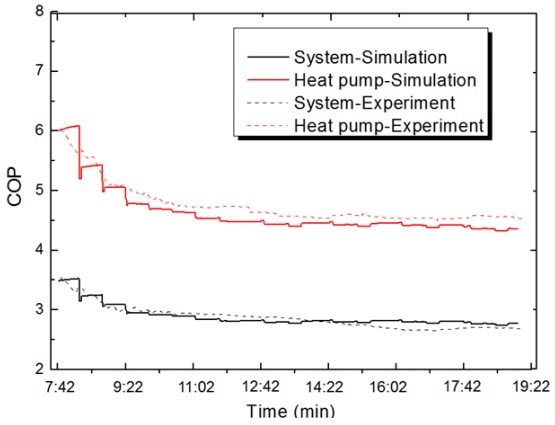

676

677 c) Instantaneous COP

678 Fig. 8 Validation results when the system operated without auxiliary cooling system.

679

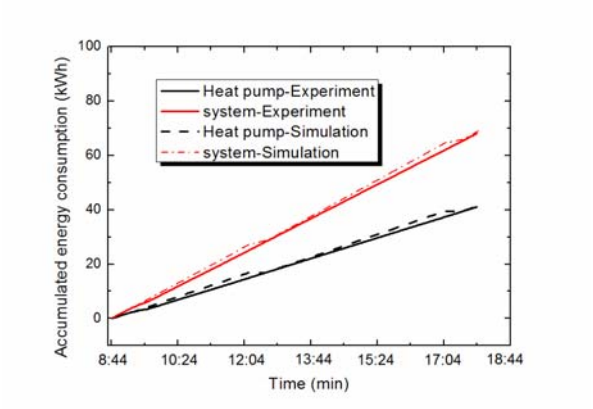

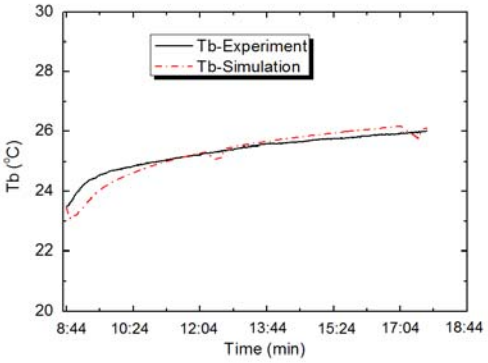

680

681 a) Accumulated power consumption b) Borehole wall temperature

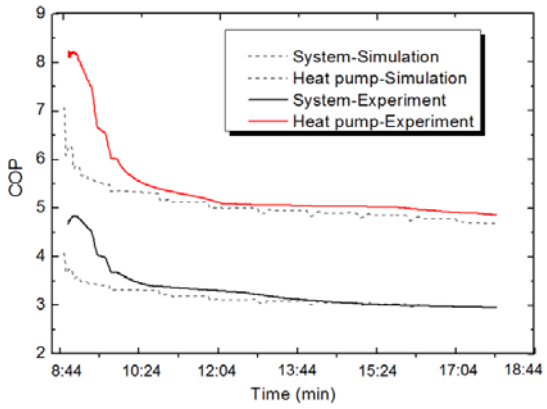

682

683 c) Instantaneous COP

684 Fig. 9 Validation results when the system operated with auxiliary cooling system.

685

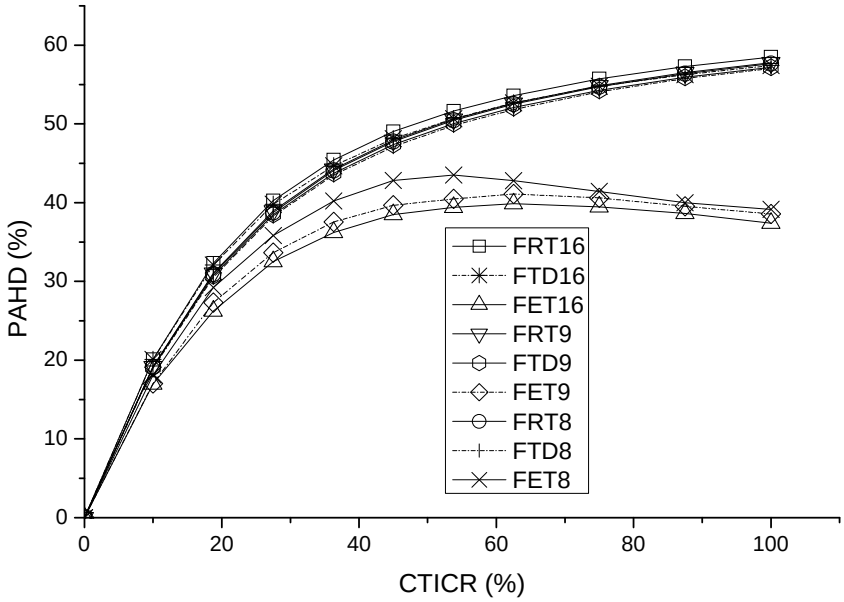

686

687 Fig. 10 The relationship between PAHD and CTICR under different system operation scenarios.

688

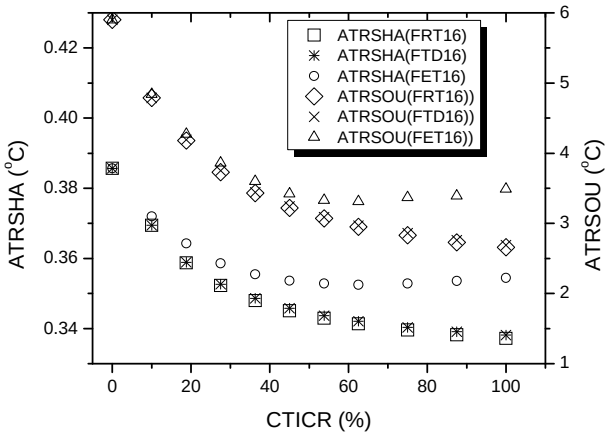

689

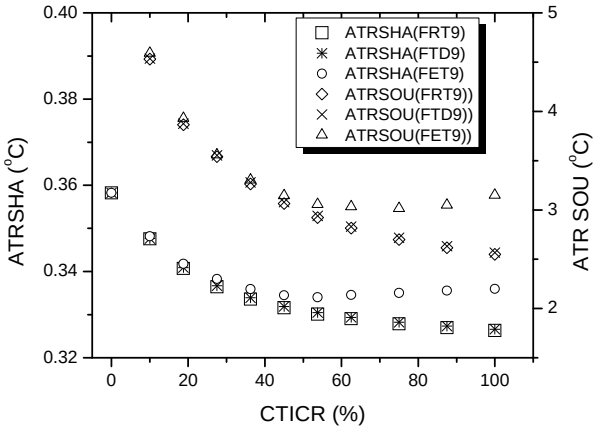

690 a) 16 hours operation b) 9 hours operation

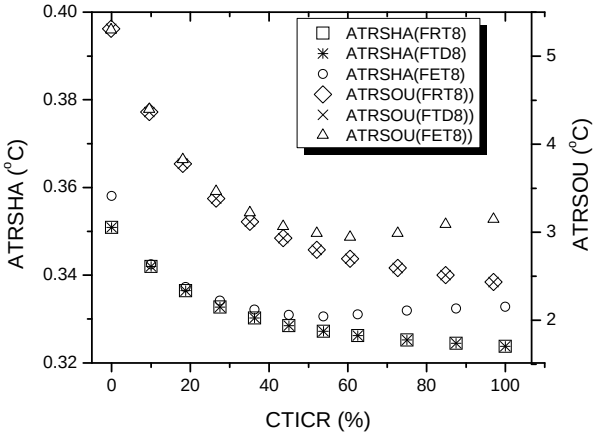

691

692 c) 8 hours operation

693 Fig. 11 The variation of ATRSHA and ATRSOU with the variation of CTICR.

694

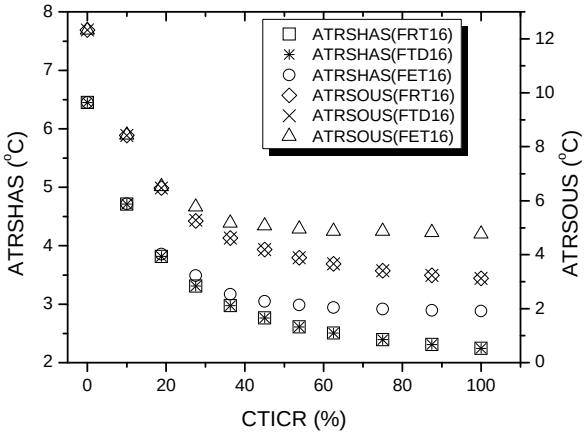

695

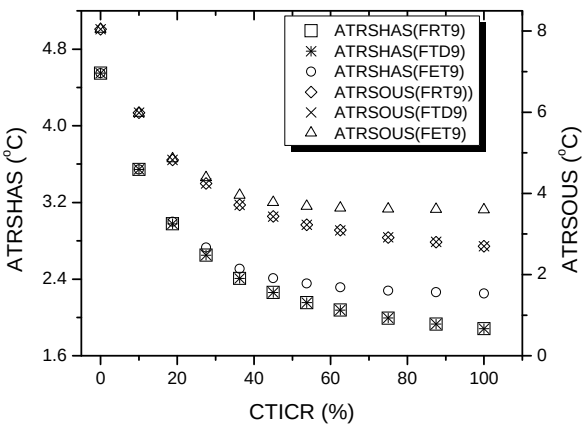

696 a) 16 hours operation b) 9 hours operation

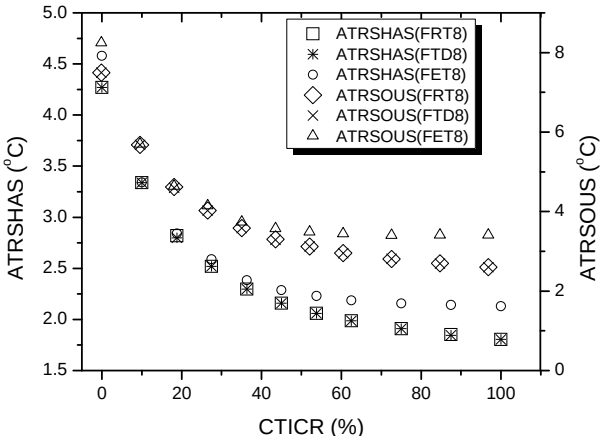

697

698 c) 8 hours operation

699 Fig. 12 The variation of ATRSHAS and ATRSOUS with the variation of CTICR in summer.

700

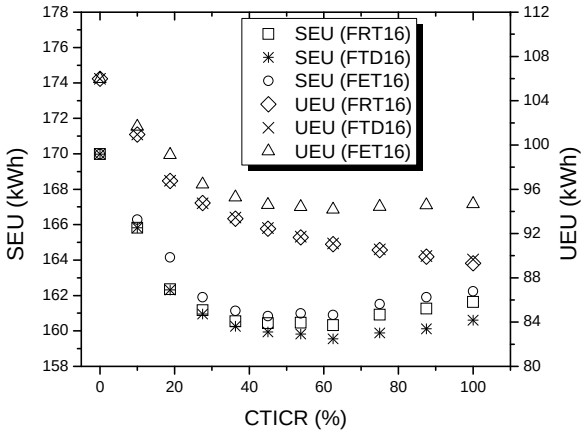

701

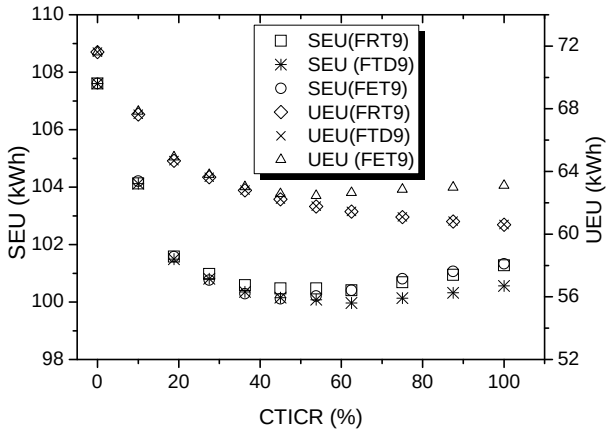

702 a)16 hours operation b) 9 hours operation

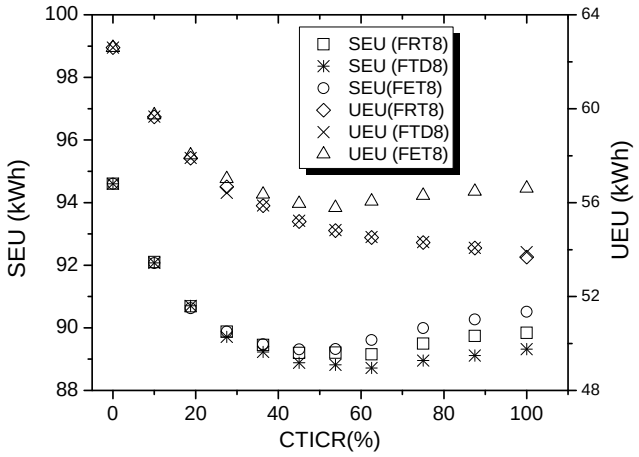

703

704 c) 8 hours operation

705 Fig. 13 The variation of SEU and UEU with the variation of CTICR.

706

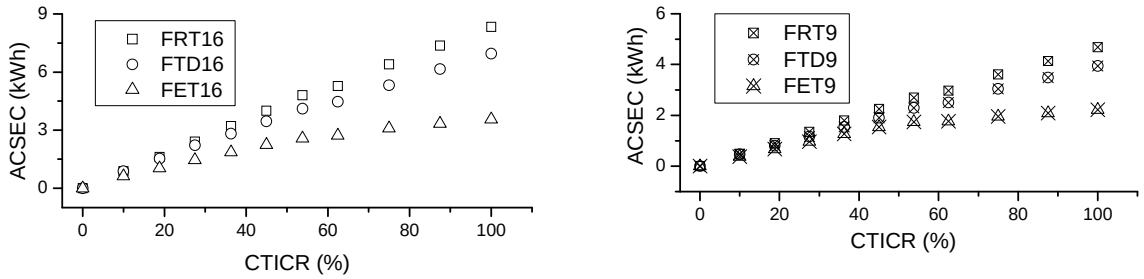

707

708 a) 16 hours operation b) 9 hours operation

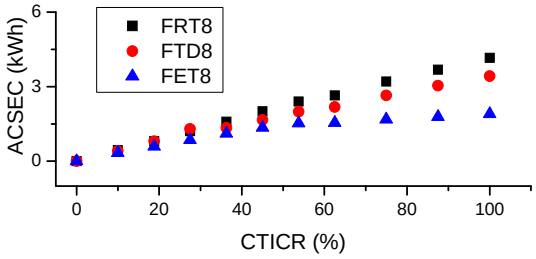

709

710 c) 8hours operation

711 Fig. 14 The variation of ACSEU with the variation of CTICR.

712

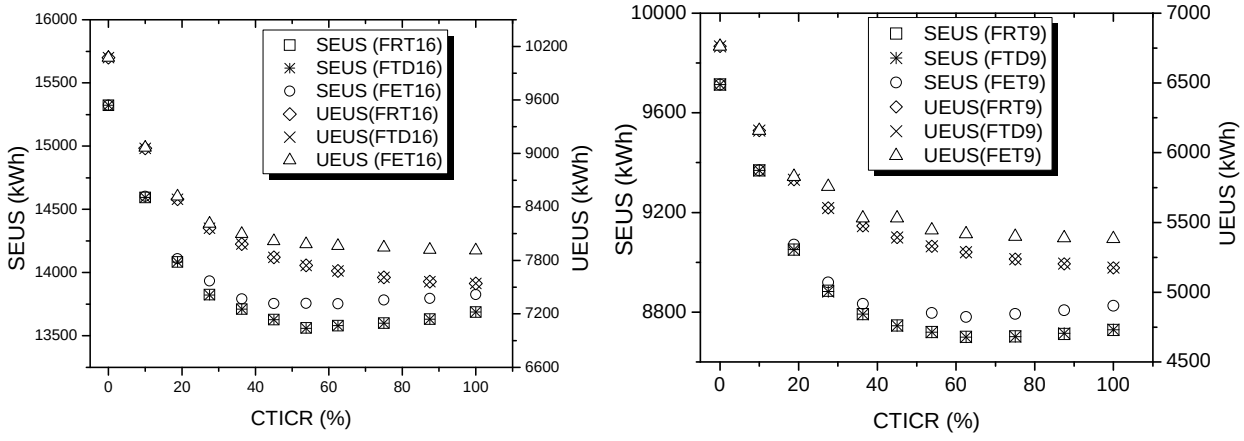

713

714 a) 16 hours operation b) 9 hours operation

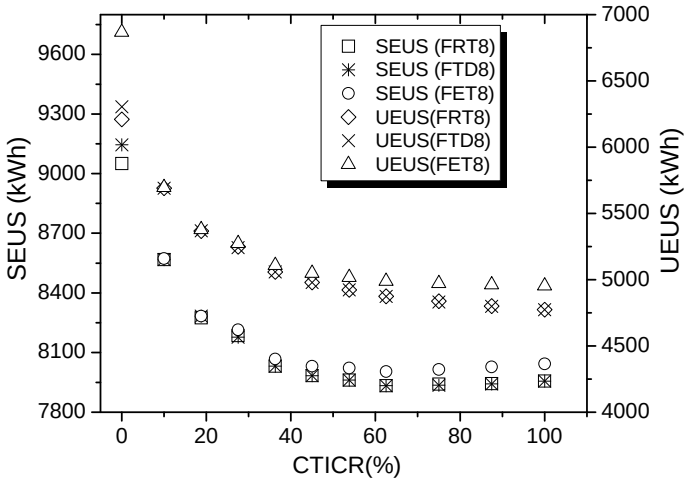

715

716 c) 8hours operation

717 Fig. 15 The variation of SEUS and UEUS with the variation of CTICR.